Acoustic-gravity Waves in Space Generated by Near-ground and Volume Sources

Elena S. Andreeva[1], **Viacheslav E. Kunitsyn**[1,2], **Ivan A. Nesterov**[1], **and Artem M. Vorontsov**[1]

[1]M.V. Lomonosov Moscow State University, Moscow, Russia
[2]Institute of Physics of the Earth, Russian Academy of Sciences, Moscow, Russia

Abstract— Numerical analysis of acoustic-gravity waves (AGW) generation and propagation in the Earth's atmosphere is performed based on computer model of stratified atmosphere with dissipation. Atmospheric and ionospheric wavelike disturbances generated by near-ground or volume sources such as oscillations of the Earth's or oceanic surface, earthquakes, explosions, seiches, tsunami waves and temperature heating are studied. These wavelike phenomena in the atmosphere and ionosphere appear as the alternating areas of enhanced and depleted density (in the atmosphere) or electron concentration (in the ionosphere).

1. INTRODUCTION

Observation and investigation of various ionospheric perturbations under assumption of their correct physical interpreting and understanding of their hydrodynamic generation mechanisms commonly allows obtaining current or predictive configuration of near-ground or volume sources of disturbances. The least studied problem here is a question about acoustic energy transferring from the ground sources into near-Earth space that primarily is related with incompleteness of AGW propagation theory in the real atmosphere. Moreover, complete analysis of the observed ionospheric perturbations should be performed using conventional characteristics of ionospheric waves such as amplitude, phase, period, velocities of corresponding wave packets and angular characteristics of the wave vector. Notice, that for most near-ground or volume sources in geophysical bibliography there is a significant variance regarding values of basic AGW parameters as well as absence of unified point of view on AGW generation mechanisms. As the examples of mentioned mechanisms different authors provide infrasound wave generation [1], internal gravity waves generation [2], eddying motion of the neutral component generated by an acoustic pulses [3], the generation of shock-acoustic waves [4], etc..

The numerical simulation of upper atmosphere responses to various near-ground or volume sources can provide estimations of basic AGW characteristics and to clarify AGW generation mechanisms. The major results of the paper consist in determining of common as well as unique tendencies in AGW behavior for a wide class of sources, analysis of these tendencies and estimation of AGW wavepackets' parameters.

2. NUMERICAL MODEL OF AGW GENERATION AND PROPAGATION IN THE UPPER ATMOSPHERE

In order to analyze the propagation conditions and mechanisms of AGW generation, we follow [5] and consider the equations of geophysical hydrodynamics:

$$\begin{aligned}
&\frac{\partial\rho}{\partial t}+\nabla\left(\rho\mathbf{v}\right)=0\\
&\rho\left(\frac{\partial\mathbf{v}}{\partial t}+\left(\mathbf{v},\nabla\right)\mathbf{v}\right)=-\nabla p+\rho\mathbf{g}+\mathbf{F}_d\\
&\rho\left(\frac{\partial\left(c_{\mathbf{v}}T\right)}{\partial t}+\left(\mathbf{v},\nabla\right)\left(c_{\mathbf{v}}T\right)\right)=-p\left(\nabla,\mathbf{v}\right)+Q_d\\
&p=\frac{\rho}{m_0}RT
\end{aligned}\tag{1}$$

Since our study addresses very fast motions that are commensurate to the propagation of AGWs, the Coriolis force is insignificant and it is neglected in our analysis. Here, ρ is density, T is temperature, p is pressure, $\mathbf{v}$ is the particle velocity in the wave, $\mathbf{g}$ is the acceleration of gravity, $\mathbf{F}_d$ is the drag force, Q_d is the absorbed heat due to wave dissipation, $c_{\mathbf{v}}$ is the specific heat of gas at constant volume, m_0 is the relative molecular mass of air, and R is the universal gas constant. This model takes into account the turbulent viscosity up to the heights of the tropopause and the iondrag, which takes place significantly above the tropopause. These dissipative forces are introduced as a single common drag force in the Rayleigh form $\mathbf{F}_d = -\alpha\mathbf{v}$. Here, α is the drag coefficient, whose values at different heights correspond to different mechanisms of dissipation.

For the numerical integration of the system (1), it is reasonable to represent each thermodynamic parameter as a sum of two parts: the stationary part and the perturbed part. Then the initial conditions for the velocity, perturbations of density, pressure and temperature can be chosen equals to zero. As the lower boundary condition, we require that the air particle velocity in the atmospheric boundary layer is equal to the velocity of motion of the Earth's surface or the ocean surface. The same condition governs the translation of the perturbation from the moving medium to the atmosphere. For the remaining unknowns, we assume that they are continuous at the transition through the lower boundary. On the upper and side boundaries the conventional boundary conditions are utilized that provide waves propagation through these surfaces without a significant reflection.

The numerical solution of the system (1) was obtained using the flux corrected transport algorithm (FCT) [6]. This method has proven to be quite efficient in the numerical solution of the similar problems of modeling the ionospheric responses to the explosions and earthquakes (see [7, 8]). We will seek the solution of this problem in a rectangular domain, assuming that the sphericity of the Earth does not affect the further results. Introduce the 2D Cartesian coordinates Oxz, in which the Ox axis is horizontal and the Oz axis is directed vertically upwards. In these coordinates, $\mathbf{r} = (x, z)$ and $\mathbf{v} = (u, w)$, where $u(w)$ is the horizontal (vertical) component of the particle motion velocity in the medium. For solving the given system by the FCT approach, we apply the method of time step splitting along the directions x and z so that righthand sides of (1) are separated into the horizontal and vertical components.

3. NUMERICAL SIMULATION RESULTS

The analysis of numerical simulation results shows the AGW presence in the atmosphere for all types of studied near-ground or volume sources of disturbances. The following general patterns of the AGW propagation in the upper atmosphere were observed for all types of sources: generation of acoustic perturbations above the epicenter of near-ground source at the heights or above of the mesopause having spatial scales about 1000 km along horizontal direction and about 400 km along vertical direction; generation of internal gravity waves (IGW) packets extending from two to several wavelengths that in the waveguide channel at the heights above the mesopause are captured and in the opposite horizontal directions from the Earth's disturbances source are propagated (for example see Figs. 1(a), (b)). Further IGW propagation is followed by increasing of their period and the wavelength with the distance from the source. At the distance about 2000 km from the epicenter of the near-ground disturbances increasing of the period was approximately 120–150 s in comparison with the value of the IGW period above the epicenter.

The atmospheric waves observed in the numerical simulations have contained both types of the AGW spectrums: acoustic and gravity parts. The periods of acoustic waves (AW) was about 170–290 s, the IGW periods — 750–1500 s. Note that during first 1000 s of perturbations' propagation the AW period was about 170–200 s and after the AW reaching at 400–500 km heights and forming of the stable acoustic response this period was increased to 220–290 s. The group velocity of the AW was varied from 340 m/s to 600 m/s depending on height above the ground, the IGW had corresponding velocities in the range 250–310 m/s that were slightly increased with the propagation

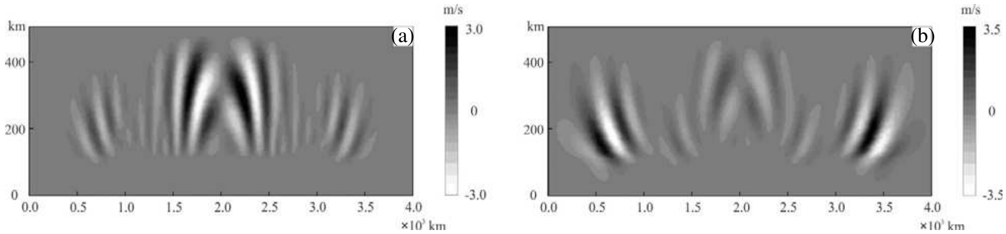

Figure 1: The spatial distributions of u at the time $t = 5500$ s after generating of (a) pulse and (b) long-period oscillations of the Earth's ground giving approximately the same amplitudes of upper atmosphere's perturbation. Here and below source of disturbances near the point $x = 2000$ km, $z = 0$ km is located.

distance. The horizontal IGW wavelength was 250–280 km, the horizontal AW wavelength was 170–200 km.

Now consider the basic properties of ionospheric responses for several examples of sources. At the beginning consider generator of short- and long-period oscillations of the Earth's ground caused by underground explosions, shallow earthquakes and so on. For the earthquakes and explosions the spectrum of atmospheric perturbation was commonly concentrated in the acoustic range with dislocation above the source (Fig. 1(a)). The amplitudes of the w in the AW above the explosion source could reach tens of meters per second. The gravity waves was poorly represented, their periods were approximately in the range 750–900 s.

For the long-period local Earth's surface oscillations the maximal amplitudes of the u and w in the AW were not more than 20–30 m/s and 10–30 m/s for the IGW. The atmospheric perturbation was commonly consists of the IGW of the periods $P > 1000$ s propagating without significant attenuation at the several hundreds of kilometers (Fig. 1(b)). The comparison analysis shows that the amplitude of the IGW in the case of long-period source is more than in the short-period case.

One more near-ground source having large enough ionospheric response is the seiches — the long-period oscillations of the water surface commonly taking place in a closed waters. The calculations show that seiches basically generate long-period AGW (Figs. 2(a), (b)). In the numerical simulations of the seiches at the Geneva lake, Baikal lake and Michigan lake [9] the amplitudes of the velocities u and w in the corresponding IGW, as the rule, were less than 1 m/s. The IGW propagation could be described in terms of wave packets going from the source with time delay 1.5–2.0 hours. The horizontal phase velocity of the IGW was in the range 280–300 m/s, the period was 900–1500 s, wavelength — 320–450 km.

The next important class of ionospheric perturbations' generators includes temperature inversions in the lower atmosphere, volcano eruptions, perturbations of incoming air flow by the "warm" megalopolises, solar heating and photo dissociation in the troposphere [10]. All mentioned phenomena have a distinguishing feature — all of them connect with local near-ground temperature variation.

The numerical simulation of the atmospheric response to the temperature variations source shows presence of large scale IGW having large amplitudes (u, $w \sim$ 30–50 m/s) and low AW response (Fig. 3(a)). In contrast with previously discussed sources in this case large temperature perturbations were observed (Fig. 3(b)). The comparison analysis has demonstrated that approximately the equivalent IGW are generated by temperature source with amplitude 0.25 K as well as are formed by long-period Earth surface's oscillations with the amplitude about ten meters and the period about 1000 s.

One more interesting example of AGW generator gives the tsunami wave propagation in the

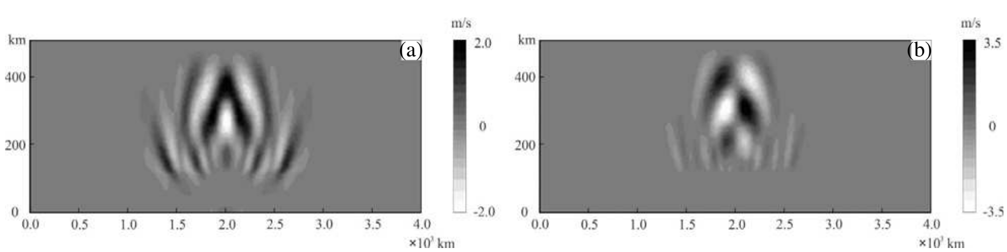

Figure 2: The spatial distributions of the velocities (a) u and (b) w at $t = 5600$ s for the numerical model of the seiches having vertical amplitude 2 m, the period 10000 s and spatial scale about 300 km.

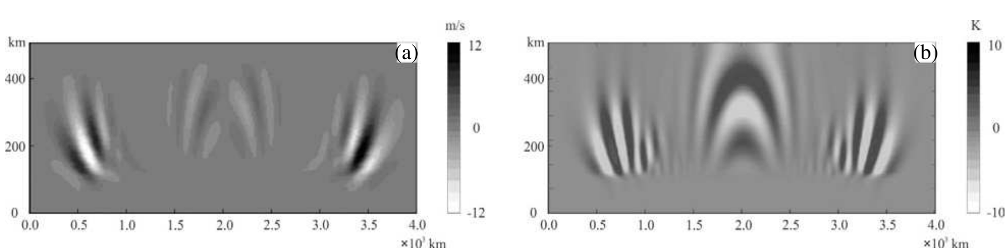

Figure 3: The spatial distribution of (a) u and (b) T at $t = 6000$ s for the temperature source with the amplitude 1 K and spatial scale 20 km. The temporal period of the source is equal to 3000 s.

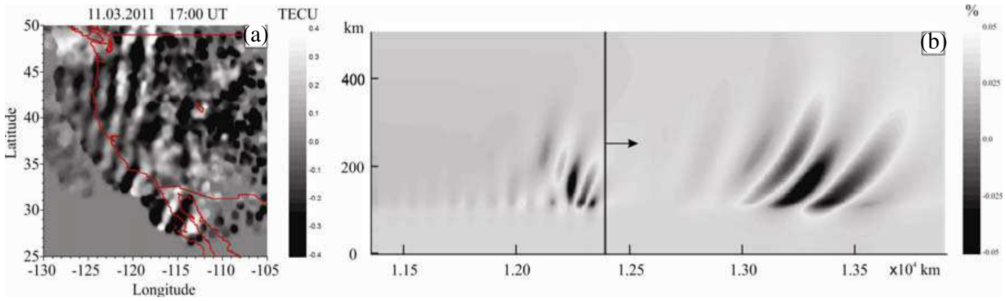

Figure 4: The TEC variation map (a) obtained by GPS RT for the west coast of the USA after 11 hours from the main shock of Tohoku earthquake. The relative density distribution ρ simulation result near the Hawaii islands (b) after 8 hours from the main shock. The position and the propagation direction of the tsunami wave are denoted by the corresponding lines.

open ocean. Consider the upper atmosphere response to the severe Tohoku earthquake of March 11, 2011. The Fig. 4(a) represents the total electron content (TEC) reconstruction in the US west coast region by the GPS radio tomography (RT) after 11 hours from the main shock. In [11] shows that ionospheric waves in this image primarily correspond to the tsunami wave propagation in the Pacific ocean. The computer simulation (Fig. 4(b)) of the tsunami-induces AGWs demonstrates a distinct precursor of the tsunami wave, which appears as a strong IGWs advancing the perturbation of the ocean surface (and the accompanying AWs) and largely concentrated in the band moving 500–1000 km ahead of the tsunami.

In conclusion, note that the presented numerical simulation results show close agreement with the experimental and theoretical researches for the corresponding sources of disturbances [3, 4].

ACKNOWLEDGMENT

The work was accomplished in the scope of the contract agreement with Russian Foundation for Basic Research (grants Nos. 13-05-01122, 14-05-00855).

REFERENCES

1. Calais, E. and J. B. Minster, "GPS, earthquakes, the ionosphere, and the Space Shuttle," *Physics of Earth and Planetary Interiors*, Vol. 105, 167–181, 1998.
2. Francis, S. H., "Global propagation of atmospheric gravity waves: A review," *J. Atmos. Terr. Phys.*, Vol. 37, 1011–1054, 1975.
3. Andreeva, E. S., M. B. Gohberg, V. E. Kunitsyn, et al., "The RT registration of ionospheric perturbations from the ground explosions," *Kosmicheskie Issledovaniya (Space Research)*, Vol. 39, No. 1, 13–17, 2001.
4. Afraimovich, E. L., N. P. Perevalova, A. V. Plotnokov, and A. M. Uralov, "The shock-acoustic waves generated by earthquakes," *Ann. Geophysicae*, Vol. 19, 395–409, 2001.
5. Grigoriev, G. I., "Acoustic-gravity waves in the Earth's atmosphere (review)," *Izvestia Vuzov. Radiophysics*, Vol. XLII, No. 1, 3–25, 1999.
6. Oran, E. S. and J. P. Boris, *Numerical Simulation of Reactive Flow*, Cambridge University Press, 2000.
7. Akhmedov, R. and V. Kunitsyn, "Simulation of the ionospheric disturbances caused by earthquakes and explosions," *Geomagnetism and Aeronomy*, Vol. 44, No. 1, 95–101, 2004.
8. Kunitsyn, V. E., S. N. Suraev, and R. R. Akhmedov, "Modeling of atmospheric propagation of acoustic gravity waves generated by different surface sources," *Moscow Univ. Phys. Bulletin*, Vol. 62, No. 2, 122–125, 2007.
9. Wuest, A. and D. M. Farmer, *Seishe*, McGraw-Hill, Encyclopedia of Science & Technology, 2003.
10. Sauli, P. and J. Boska, "Tropospheric events and possible related gravity wave activity effects on the ionosphere," *J. Atmos. Sol.-Terr. Phys.*, Vol. 63, 945–950, 2001.
11. Kunitsyn, V. E. and A. M. Vorontsov, "Modeling the ionosphericpropagation of acoustic gravity waves from the Tohoku tsunami of 2011," *Moscow Univ. Phys. Bulletin*, Vol. 69, No. 3, 263–269, 2014.